Deep defects and the attempt to escape frequency in organic photovoltaic materials

John A. Carr,[1] Moneim Elshobaki,[2,3] and Sumit Chaudhary[2,4,a)]
[1]*NASA–Marshall Space Flight Center, Huntsville, Alabama 35812, USA*
[2]*Department of Materials Science and Engineering, Iowa State University, Ames, Iowa 50011, USA*
[3]*Department of Physics, Mansoura University, Mansoura 3551 6, Egypt*
[4]*Department of Electrical and Computer Engineering, Iowa State University, Ames, Iowa 50011, USA*

(Received 13 June 2015; accepted 8 November 2015; published online 18 November 2015)

Trap states are well-known to plague organic photovoltaic devices and their characterization is essential for continued progress. This letter reports on both the deep trap profiles and kinetics of trap emission, studied through temperature dependent capacitance measurements. Three polymer based systems relevant to photovoltaics, namely, P3HT:$PC_{60}BM$, PTB7:$PC_{70}BM$, and PCDTBT:$PC_{70}BM$ were investigated. Each polymer showed a markedly different deep trap profile, varying in shape from a nearly constant density of states to a sharp Gaussian. In contrast, the frequency of trap emission was similar for each—ca. $10^8 - 10^9$ Hz—indicating a universal value and similar trapping mechanisms despite the differences in energetic distribution. The latter result is important in the light of range of conflicting values reported, or higher value (10^{12} Hz) typically borrowed from crystalline inorganic materials. © *2015 AIP Publishing LLC*.
[http://dx.doi.org/10.1063/1.4936160]

Organic semiconductors have been witnessing immense research activity for several device technologies. Among other physical characteristics of organic semiconductors, energetic trap sates within their band-gaps especially are in need of better understanding as they intricately affect several device properties and performance.[1] Herein, we investigate deep trap profiles of three contemporary polymers employed in organic photovoltaics (OPV); we specifically visit their characteristic trap emission parameter, known as the attempt to escape frequency. The attempt to escape frequency defines the dynamics of trap emission and defines the maximum rate of detrapping cycles. This frequency is quantified by

$$\nu_0 = \langle v_{th} \rangle \sigma_{p,n} N_{v,c}, \tag{1}$$

where $\langle v_{th} \rangle$ is the thermal velocity, $\sigma_{p,n}$ is the capture cross section, N is the relevant band density of states (DOS) and $\nu_0 = \omega_0/2\pi$.[2,3] All models related to detrapping dynamics require ν_0. For example, ν_0 defines the demarcation energy in admittance spectroscopy based defect measurements. Thermal emission of a hole trapped in a defect with activation energy E_a is given by[2–5]

$$e_p = N_v \langle v_{th} \rangle \sigma_p \exp\left(\frac{-E_a}{k_B T}\right). \tag{2}$$

There has been little work to quantify ν_0 for organic semiconductors. Most studies have borrowed values ($10^{11} - 10^{13}$ Hz) from inorganics,[6–12] or left the parameter unknown.[13] Few works have measured ν_0 in organic semiconductors. In the PPV based solar cells and diodes, values between 10^7 and 10^8 Hz were reported.[14,15] One report[16] has ν_0 of 5×10^{12} Hz for pentacene thin-films and another[17] has found 10^5 Hz for sexithiophene based transistors. A recent report found $\nu_0 = 33.4$ Hz for polyhexylthiophene (P3HT).[18] Clearly, a large range of values—10^1 to 10^{14} Hz—indicate either unique values for different materials, or discrepant measurements.

Neglecting degeneracy, emission of a trapped hole is defined by Eq. (2). In this Arrhenius relationship, emission rate depends on the trap depth, sample temperature and the pre-exponential factor, $N_v \langle v_{th} \rangle \sigma_p$, or collectively, ν_0.[2,3,19] Linearizing Eq. (2) yields

$$\ln(e_p) = -\frac{E_a}{k_B T} + \ln(\nu_0), \tag{3}$$

where an Arrhenius plot of the $\ln(e_p)$ vs. $1/T$ gives a straight line with a slope that defines the trap activation energy and an intercept that defines ν_0.[2] Thus, by monitoring the change in trap emission with a change in sample temperature, ν_0 can be obtained. This treatment assumes the pre-exponential factor to be temperature independent. However, in inorganic materials, N_v and $\langle v_{th} \rangle$ are known to vary proportionally with $T^{3/2}$ and $T^{1/2}$, respectively, giving a temperature dependence to ν_0.[5] To account for this, the prefactor is sometimes written as "ΥT^2" where $\Upsilon = N_v \langle v_{th} \rangle \sigma_p T^{-2}$, and then the $\ln(e_p/T^2)$ is plotted vs. $1/T$ to determine its value.[4,5] However, since the T term within the exponential dominates T^2 term, the calculated frequency is not much different and the temperature dependence is often neglected.[2] Nonetheless, results were analyzed both ways herein.

The change in trap emission with a change in temperature can be tracked through capacitance measurements. It is well known that semiconductor devices have a depletion region that displays parallel plate like capacitance, called the depletion capacitance (C_d).[3,5] Deep-trap states augment this capacitance by changing their occupancy as a function of the small signal frequency or DC voltage.[2,3,5,20] Consider a one-sided junction rich in deep-defect states (in this report, the

a)sumitc@iastate.edu

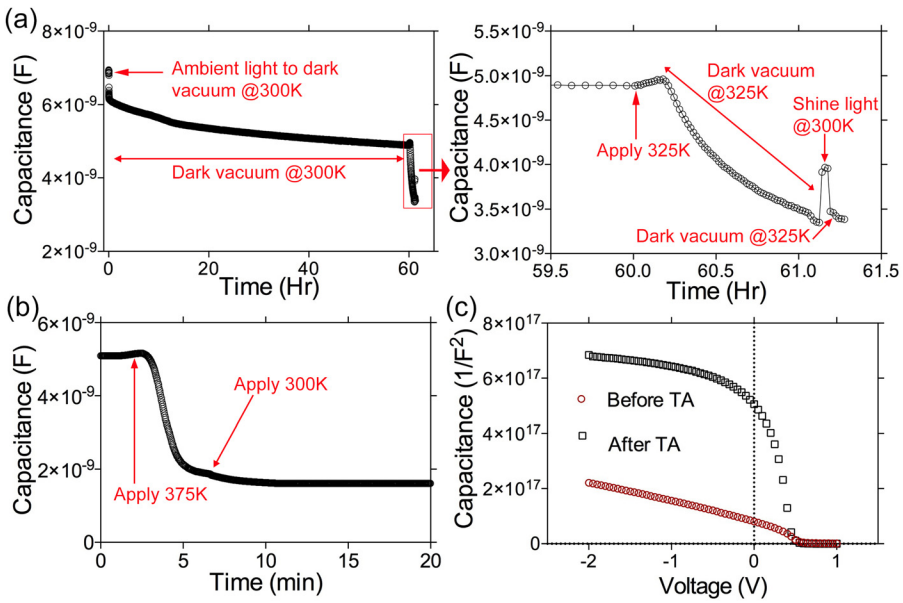

FIG. 1. (a) Effects of the vacuum environment on the capacitance of a P3HT:PC_{60}BM device. Device was in the dark at 300 K and data was taken at 10 kHz. (b) Effects of 375 K stabilization on the capacitance of a P3HT:PC_{60}BM OPV in the cryo vacuum. Data was taken at 10 kHz. (c) Mott-Schottky representation of CV data taken before and after thermal annealing (TA). Data was taken at 200 kHz.

metal-semiconductor junction). As a small AC signal superimposed atop a 0 V DC bias, the capacitance of the junction responds according to the applied frequency. As the frequency is swept from high frequency (few traps responding) to low frequency (most traps responding), "steps" are seen in the capacitance. Corresponding peaks in the differential $-FdC/dF$ display Arrhenius behavior with changing temperature.[2,5] Due to the demarcation of AC signal, the frequency of these peaks represents the emission rate of the responding trap. Thus, by plotting the frequency at which the peak occurs vs. $1/T$, ν_0 is found through Eq. (3).[2,5] Capture cross section is then obtained through Eq. (1) and, coupled with the formalism of Walter *et al.*,[2] the deep trap profile is depicted. The subsequent paragraphs detail ν_0 and deep trap profile measurements for P3HT, PTB7 (Poly[[4,8-bis[(2-ethylhexyl)oxy]-benzo[1,2-b:4,5-b′]dithiophene-2,6-diyl][3-fluoro-2-[(2-ethylhexyl)carbonyl]thieno[3,4-b]thiophenediyl]]), and PCDTBT (poly[N-9′-heptadecanyl-2,7-carbazole-alt-5,5–(4′,7′-di-2-thienyl-2′,1′,3′-benzothiadiazole)]) blended with fullerene-derivatives. Temperature dependent capacitance-frequency (CF) measurements were performed in a liquid nitrogen cryostat (Fig. S1).[21] To ensure validity, the system was benchmarked with measurements on amorphous silicon solar cells (Fig. S2).[21]

We begin with the results for P3HT:PC_{60}BM devices. PV performance is shown in Table S1 and Fig. S3.[21] Interestingly, these devices needed stabilization in the cryostat vacuum environment. The need for stabilization was found empirically as data at 300 K before and after the low temperature experiments did not line up. To probe this issue, capacitance of P3HT:PC_{60}BM devices was monitored over time in vacuum. Fig. 1(a) shows an example at 300 K and 10 kHz for 50+ h. Capacitance drops significantly over time, which will clearly affect the validity of successive CF measurements, resulting into erroneous deduction of ν_0. At 300 K, the capacitance was unstable even after 50 h. 325 K was then applied to the device. An initial increase in the capacitance was first seen, corresponding to an increase in the response of trap states, followed by a rapid decrease. To determine if the decrease was caused by the release of deeply stored photocharge, samples were illuminated at 300 K and then returned to dark vacuum at 325 K. As expected, capacitance increased and then quickly decreased. However, its value did not reach the original value, indicating another mechanism behind the capacitance behavior over the 61 h experiment. The sample encountered no low temperatures during this measurement, leaving only the possibility of environmental change.

It is known that P3HT films de-dope in vacuum due to desorption of oxygen.[22] This occurs in the timeframe of weeks at 300 K to a few minutes at higher temperatures (e.g., 370 K).[22] To test this likely explanation behind reduced capacitance over time, capacitance of a P3HT:PC_{60}BM device was monitored in vacuum at 375 K (Fig. 1(b)). Capacitance-voltage (CV) doping data was taken before and after (Fig. 1(c)). The 375 K treatment led to a rapid decrease in capacitance within a few minutes, with the drop being larger than both the 300 K and 325 K treatments. After returning to 300 K, the capacitance stabilized and remained so thereafter. A large decrease in the measured free charge carriers was noted, from 3.0×10^{16} cm^{-3} before to 7.0×10^{15} cm^{-3} after the thermal treatment, which supports oxygen desorption and removal of related defects. Thus, it is evident that vacuum measurements on organic materials must be carefully monitored and stabilized to ensure accuracy. All P3HT devices herein were thermally treated in vacuum at either 375 K (<10 min) or 325 K (ca. 20 h).

Fig. 2(a) shows CF data for P3HT:PC_{60}BM devices. CF plots shift as a function of temperature. Below 200 K, geometric capacitance appears as the freeze-out is reached. Extending from this geometric capacitance, there is a step in the capacitance from ca. 1.75 nF to ca. 2.75 nF. Peaks in the FdC/dF differential shift to lower frequencies at lower temperatures (Fig. 2(b)). The peak frequencies are plotted vs. $1/T$ in Fig. 2(c). A straight line is revealed by the Arrhenius plot, yielding ν_0 of 1.2×10^9 Hz and an activation energy of 210 meV. This value is in contrast to a previously reported one (33.4 Hz),[18] but in line with data for PPV based devices.[14,15] Assuming a $\langle v_{th} \rangle = 10^7$ cm/s and $N_v = 10^{19}$ cm^{-3}, a capture cross section of 1.2×10^{-17} cm^2 was calculated.

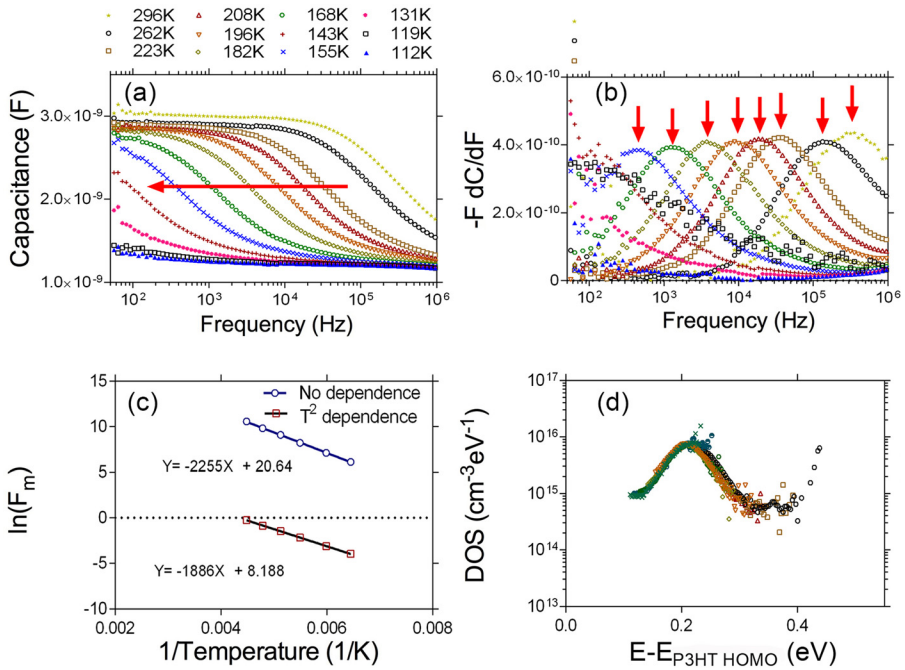

FIG. 2. P3HT:$PC_{70}BM$: (a) Capacitance vs. frequency as a function of temperature. The red arrow indicates the Arrhenius shift of a trap band with lowering temperatures. (b) $-FdC/dF$ differential. Arrows indicate emission peaks. (c) Arrhenius plot of the $-FdC/dF$ peak frequencies versus $1/T$. (d) tDOS profiles at different temperatures.

Fig. 2(d) shows the corresponding trap DOS (tDOS) profiles based on formalism by Walter *et al.*[2] (this formalism deduces energy distribution of defects by measuring complex admittance of a junction). The tDOS shape is in agreement with profiles found elsewhere, with the shift of the profile in the x-axis energy corresponding to the newly measured ν_0.[6,10,23] The measured ν_0 gives good overlap in the tDOS profile of the individual temperatures (Fig. 2(d)), while a prefactor two orders of magnitude lower (Fig. S6(b)) or higher (Fig. S6(c)) skews the results. A dominant band at 210 meV can be seen. In previous works,[6,10,23] this first step was referred to as a deep defect band; however, this temperature data indicates this band is better described as the free carrier response band, i.e., a step in capacitance from $C_d = \epsilon_s\epsilon_0 A/t$ to $C_d = \epsilon_s\epsilon_0 A/W$,[5] where W is depletion width. This response band is expected to have a thermal activation energy similar to the difference between the Fermi-level and the HOMO of the polymer. The measured 210 meV corresponds well to the Fermi-level (220 meV from HOMO) calculated from the doping measured by CV data (2.0×10^{15} cm^{-3}). At higher energies, deeper defect states are revealed and the beginning of a second Gaussian can be seen.[23] Analysis of the temperature data between 0.25 eV and 0.35 eV shows a lower ν_0 of around 1.0×10^8 Hz. This indicates that the carrier response band and deeper defects do not share the same prefactor. Table I summarizes the experimental data. One notes the reduction of measured traps in this device compared to our previous defect work.[23] This is likely the result of thermal stabilization, which will remove both oxygen and structural based defects.

TABLE I. Summary of temperature dependent CF data.

Polymer	ν_0 (Hz)	σ (cm^2)[a]
P3HT	1.0×10^8	1.0×10^{-18}
PTB7	5.0×10^7	5.0×10^{-19}
PCDTBT	4.5×10^9	4.5×10^{-17}

[a]Literature values $\langle v_{th} \rangle = 10^7$ cm/s and $N_v = 10^{19}$ cm^{-3} were assumed for these calculations; thus the value of σ is subject to error (likely underestimated, considering the low values of σ).

Fig. 3 shows the CF data for PTB7:$PC_{70}BM$ devices. PV performance is shown in Table S2 and Fig. S4.[21] Interestingly, these devices did not need stabilization in the vacuum environment. Fig. S7 compares capacitance vs. time for P3HT and PTB7 OPVs.[21] No decrease in the PTB7 capacitance or change in the free carrier density was recorded. The reason for this difference is unknown. Fig. 3(a) shows sample temperature dependent CF data for these devices; a clear shift in the capacitance with decreasing temperature is seen. Again, there was somewhat sharp step followed by a slower increase in the capacitance. Fig. 3(b) shows the corresponding FdC/dF peaks and Fig. 3(c) the Arrhenius plot of these peaks. ν_0 of 2.3×10^8 Hz with an activation energy of 170 meV was found. Capture cross section of 2.3×10^{-18} cm^2 is then calculated. As this capacitance step starts at the geometric value, it again likely corresponds to the carrier response band. The measured activation energy (170 meV) closely matches the Fermi-level (160 meV) calculated from the doping extracted from the CV data (2.0×10^{16} cm^{-3}). Fig. 3(d) shows the corresponding tDOS profiles. A clear carrier response Gaussian at about 170 meV leads into deeper states, which only slightly increases at deeper energies. Interestingly, the deep defect profile in PTB7 devices was notably different from P3HT, a nearly constant distribution in PTB7 compared to a clear Gaussian in P3HT. Careful analysis of the temperature data between 0.15 eV and 0.25 eV again shows a slightly lower prefactor for the deeper states, about 5.0×10^7 Hz. Table I summarizes the experimental data.

Fig. 4 shows the CF data for PCDTBT:$PC_{70}BM$ devices. PV performance is shown in Table S3 and Fig. S5.[21] Interestingly, these devices also needed no stabilization in vacuum. Fig. S8 shows capacitance vs. time for P3HT, PTB7, and PCDTBT based devices. Fig. 4(a) shows the temperature dependent data for a PCDTBT device. A shift in capacitance with temperature is seen. The capacitance increase

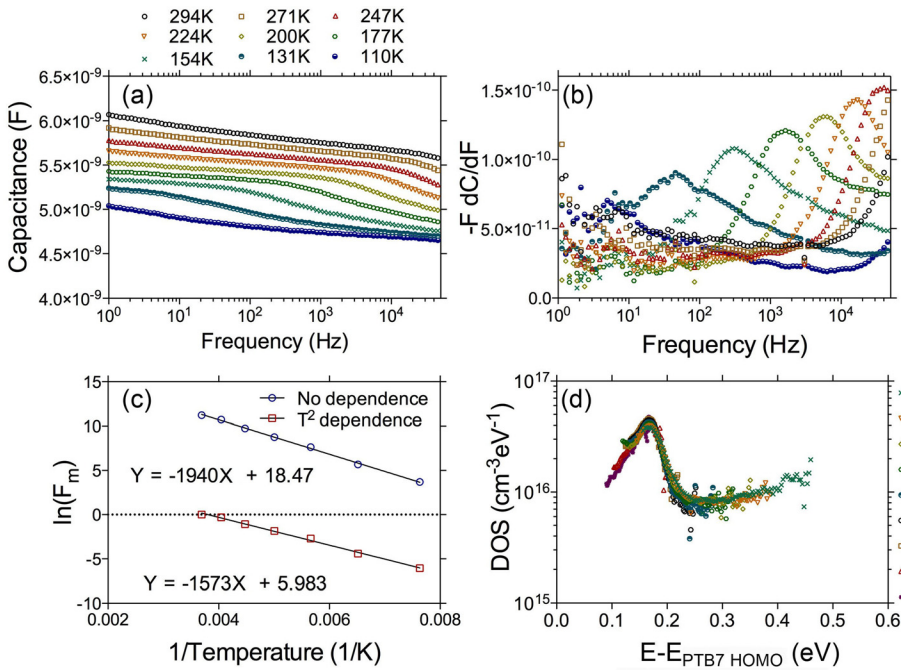

FIG. 3. PTB7:$PC_{70}BM$: (a) Capacitance vs. frequency as a function of temperature. (b) $-FdC/dF$ differential. (c) Arrhenius plot of the $-FdC/dF$ peak frequencies versus $1/T$. (d) tDOS profiles at different temperatures. At frequencies higher than shown, capacitance increased exponentially with large dissipation factors (>10); that data was excluded.

is largely broad; however, a subtle step is noted around 5.8 to 5.9 nF. The FdC/dF differentials have weak peaks (Fig. 4(b)). The peak frequencies are plotted vs. $1/T$ in Fig. 4(c), revealing ν_0 of 4.5×10^9 Hz, activation energy of 358 meV and capture cross-section of 4.5×10^{-17} cm^2. Clearly, this capacitance step does not originate at the geometric capacitance, indicating that this is a deep defect band, shifting the capacitance to $C_d = \epsilon_s \epsilon_0 / A\langle x \rangle$,[5] where $\langle x \rangle$ represents the first moment of charge response or the center of gravity of the charge response. Fig. 4(d) shows the tDOS profiles. The deep Gaussian defect is revealed around 360 meV while the carrier response band starts appearing at lower energies. Doping of 1.0×10^{16} cm^{-3} was calculated from the CV data, putting the Fermi-level at ca. 180 meV. Table I summarizes the values of different parameters.

In summary, the deep trap profiles and pre-exponential factor (ν_0) of trap emission in different OPV materials were investigated using temperature dependent CF measurements. These measurements are sensitive to the fidelity of cryogenic systems, driving the need for careful calibration and benchmarking. The system used was benchmarked with the well-known amorphous-silicon solar cells, showing its accuracy and the validity of presented results. Three polymer systems were studied: namely, (i) P3HT:$PC_{60}BM$, (ii) PTB7:$PC_{70}BM$, and (iii) PCDTBT:$PC_{70}BM$. Each was found to have ν_0 in the range of $10^8 - 10^9$ Hz, yielding capture cross sections in the range of $10^{-17} - 10^{-18}$ cm^2. Using the formalism of Walter *et al.*, deep trap profiles of these devices were extracted. Each polymer showed a carrier response band at lower energies, and a unique distribution of deep defects at higher energies. In

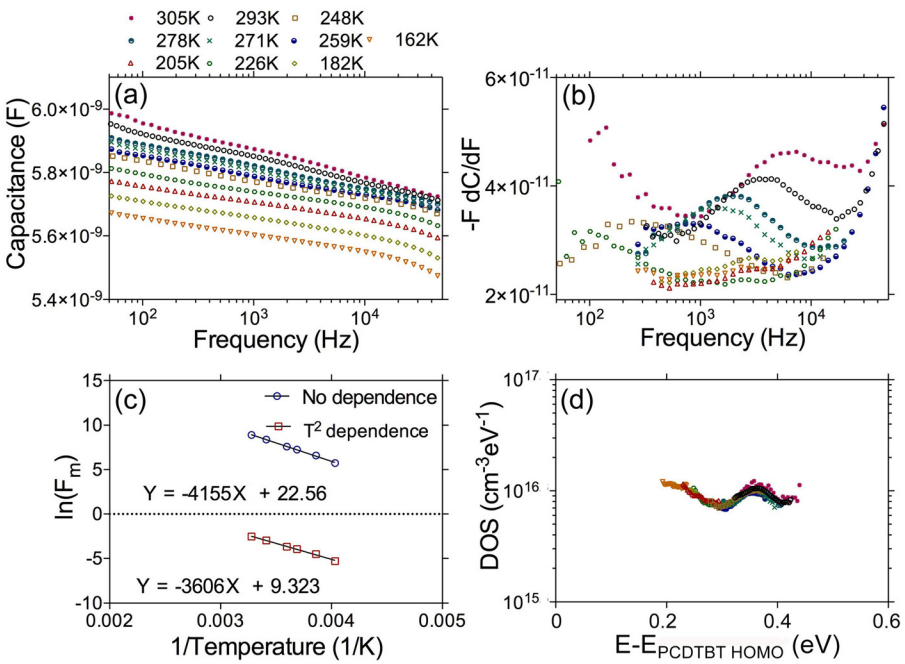

FIG. 4. PCDTBT:$PC_{70}BM$: (a) Capacitance vs. frequency as a function of temperature. (b) $-FdC/dF$ differential. (c) Arrhenius plot of the $-FdC/dF$ peak frequencies versus $1/T$. (d) tDOS profile at different temperatures.

P3HT, a brief area of constant DOS trailing to a sharp Gaussian was seen. PTB7 showed a nearly constant DOS, with a slight rise towards the deeper energies, and PCDTBT showed a clear, complete Gaussian in the deep states. Though the deep trap profiles were notably different, values of ν_0 were similar. This similarity in values of ν_0 and capture cross-sections indicates a universal value and similar trapping mechanism in conjugated polymers.

This work was supported by the U.S. National Science Foundation (ECCS-1055930). M.E. thanks Egyptian government for fellowship support (Contract No. GM915).

[1]J. A. Carr and S. Chaudhary, Energy Environ. Sci. **6**, 3414 (2013).
[2]T. Walter, R. Herberholz, C. Müller, and H. Schock, J. Appl. Phys. **80**, 4411 (1996).
[3]S. S. Hegedus and E. Fagen, J. Appl. Phys. **71**, 5941 (1992).
[4]V. Dyakonov, I. Riedel, C. Deibel, J. Parisi, C. J. Brabec, N. S. Sariciftci, and J. C. Hummelen, Mat. Res. Soc. Symp. Proc., **665**, 1–12 C7 (2001).
[5]J. Heath and P. Zabierowski, "Chapter 4: Capacitance Spectroscopy of Thin-Film Solar Cells," in *Advanced Characterization Techniques for Thin Film Solar Cells*, edited by D. Abou-Ras, T. Kirchartz, and U. Rau (Wiley-VCH Verlag GmbH & Co. KGaA, Weinheim, Germany, 2002).
[6]P. P. Boix, G. Garcia-Belmonte, U. Munecas, M. Neophytou, C. Waldauf, and R. Pacios, Appl. Phys. Lett. **95**, 233302 (2009).
[7]J. Bhattacharya, R. Mayer, M. Samiee, and V. Dalal, Appl. Phys. Lett. **100**, 193501 (2012).
[8]J. A. Carr, K. S. Nalwa, R. C. Mahadevapuram, Y. Chen, J. Anderegg, and S. Chaudhary, ACS Appl. Mater. Interfaces **4**, 2831 (2012).
[9]N. Craciun, J. Wildeman, and P. W. M. Blom, Phys. Rev. Lett. **100**, 56601 (2008).
[10]K. S. Nalwa, R. C. Mahadevapuram, and S. Chaudhary, Appl. Phys. Lett. **98**, 093306 (2011).
[11]T. Okachi, T. Nagase, T. Kobayashi, and H. Naito, Appl. Phys. Lett. **94**, 043301 (2009).
[12]H. Martens, P. W. M. Blom, and H. Schoo, Phys. Rev. B **61**, 7489 (2000).
[13]B. Ecker, J. C. Nolasco, J. Pallarés, L. F. Marsal, J. Posdorfer, J. Parisi, and E. von Hauff, Adv. Funct. Mater. **21**, 2705 (2011).
[14]V. Dyakonov, D. Godovsky, J. Meyer, J. Parisi, C. Brabec, N. Sariciftci, and J. Hummelen, Synth. Met. **124**, 103 (2001).
[15]A. Campbell, D. Bradley, E. Werner, and W. Brütting, Synth. Met. **111**, 273 (2000).
[16]V. Nadazdy, R. Durny, J. Puigdollers, C. Voz, S. Cheylan, and K. Gmucová, Appl. Phys. Lett. **90**, 092112 (2007).
[17]H. L. Gomes, P. Stallinga, F. Dinelli, M. Murgia, F. Biscarini, D. M. De Leeuw, T. Muck, J. Geurts, L. W. Molenkamp, and V. Wagner, Appl. Phys. Lett. **84**, 3184 (2004).
[18]P. P. Boix, J. Ajuria, I. Etxebarria, R. Pacios, and G. Garcia-Belmonte, Thin Solid Films **520**, 2265 (2011).
[19]J. D. Cohen and D. V. Lang, Phys. Rev. B **25**, 5321 (1982).
[20]L. Kimerling, J. Appl. Phys. **45**, 1839 (1974).
[21]See supplementary material at http://dx.doi.org/10.1063/1.4936160 for experimental details and additional figures/discussion.
[22]H. H. Liao, C. M. Yang, C. C. Liu, S. F. Horng, H. F. Meng, and J. T. Shy, J. Appl. Phys. **103**, 104506 (2008).
[23]J. A. Carr and S. Chaudhary, J. Appl. Phys. **114**, 064509 (2013).